Oxidation of stepped Pt(111) studied by x-ray photoelectron spectroscopy and density functional theory

Jochen Bandlow, Payam Kaghazchi, and Timo Jacob*
Institut für Elektrochemie, Universität Ulm, Albert-Einstein-Allee 47, D-89069 Ulm, Germany

C. Papp,[1] B. Tränkenschuh,[1] R. Streber,[1] M. P. A. Lorenz,[1] T. Fuhrmann,[1] R. Denecke,[2] and H.-P. Steinrück[1,†]
[1]*Lehrstuhl für Physikalische Chemie II, Universität Erlangen-Nürnberg, Egerlandstr. 3, D-91058 Erlangen, Germany*
[2]*Wilhelm-Ostwald-Institut für Physikalische und Theoretische Chemie, Universität Leipzig, Linnestr. 2, D-04103 Leipzig, Germany*
(Received 19 March 2011; published 11 May 2011)

In this comparative density functional theory and x-ray photoelectron spectroscopy study on the interaction of oxygen with stepped Pt(111) surfaces, we show that both the initial adsorption and oxidation occur at the steps rather than terraces. An equivalent behavior was observed for the oxide formation at higher chemical potentials, where, after the formation of a one-dimensional PtO_2-type oxide at the steps, similar oxide chains form on the (111) terraces, indicating the initial stages of bulk oxide formation.

DOI: 10.1103/PhysRevB.83.174107 PACS number(s): 81.65.Mq, 68.35.Md, 74.62.Dh, 82.80.Pv

I. INTRODUCTION

Platinum is one of the most prominent examples of a heterogeneous catalyst and is used in a wide range of industrially important reactions such as O removal reactions (e.g., CO oxidation),[1] reduction of pollutants from automobile exhaust gases (e.g., NO decomposition),[2] or O_2 reduction in fuel cells.[3] In order to understand the catalytic behavior of catalyst surfaces as well as the mechanisms behind a particular reaction, detailed knowledge of the surface morphology and electronic structure is required. However, both realistic catalysts and even model single-crystal surfaces are not completely perfect, but also involve a certain amount of step edges or other lower-coordinated surface sites. Thus, in order to gain a detailed understanding of the specific properties of platinum for oxidation reactions, one has to investigate the role of terrace *and* step-edge sites.

In the past, model studies of catalytically relevant transition metals were mostly restricted to simple planar surfaces.[4–10] Although stepped surfaces can provide a better atomistic model of real catalysts, only very recently focused experimental and theoretical efforts have been undertaken to elucidate the influence of steps on the adsorption of oxygen (or oxidation) over surfaces.[11–14]

Low-energy electron diffraction (LEED) measurements by Norton *et al.* showed that, on flat Pt(111), adsorption of oxygen from molecular beams leads to the formation of a $p(2 \times 2)$-O overlayer [at a coverage of 0.25 monolayers (ML)].[15] A combined density functional theory (DFT) and scanning tunneling microscopy (STM) study using a source of atomic oxygen has shown that (i) for coverages above 0.25 ML, a $p(2 \times 1)$-O adlayer begins to form in coexistence with the already mentioned $p(2 \times 2)$-O phase, (ii) at 0.5 ML the $p(2 \times 1)$-O structure dominates, and (iii) above 0.5 ML, one-dimensional (1D) PtO_2-oxide chains form, which preserve the $p(2 \times 1)$ superstructure.[5] These Pt-oxide chains were discussed as a potential precursor for the formation of two-dimensional or even three-dimensional surface or bulk oxides.[5]

The initial stage of oxidation of stepped Pt surfaces has also been characterized to be the formation of 1D PtO_2 structures. Using core-level spectroscopy and DFT, Wang *et al.* found the formation of a step-edge oxide at the {111}-type steps of Pt(332) surfaces,[1] which is reduced preferentially, i.e., is more reactive, compared to terrace oxygen.[1,16] Very similar structures have also been observed on Pt(110)[17] and low-index surfaces of Rh, Ru, and Pd.[18] Besides these surface oxides on pure metallic substrates, recent theoretical investigations of low-index α-PtO_2, β-PtO_2, and PtO bulk-oxide surfaces revealed high stabilities for surfaces exposing similar 1D PtO_2 oxide chains.[19] While the previous studies focused on the surface morphology, the important role of step edges for catalytic reactions has been shown for the O_2 dissociation on Pt[9(111) × (111)] and Pt[8(111) × (100)] by comparative thermal energy atom scattering, STM, and DFT studies.[20]

Despite considerable efforts, a systematic approach combining both theory and experiments to study the stability over a wide coverage range is still missing for stepped platinum surfaces; in particular, the role of differently oriented steps is not clear.[21–23]

II. EXPERIMENTAL AND CALCULATIONAL DETAILS

In the present work, the oxygen adsorption and initial stages of oxide formation on stepped Pt(111) surfaces are investigated in a systematic approach by combining DFT calculations[24] with *in situ* high-resolution x-ray photoelectron spectroscopy (XPS) experiments,[25] using a supersonic molecular beam for gas dosing.

The comparison of different stepped Pt(111) surfaces allows to elucidate the role of steps and thus helps to bridge the structure gap between simple model systems and real catalysts. Our DFT calculations allow to not only interpret the experimentally observed behavior, but also to make predictions about the surface oxidation state at high coverages (e.g., at elevated pressures), i.e., to bridge the pressure gap.

The formation energy of a stepped surface is mainly dominated by contributions from terraces, isolated steps, step-step interactions, and strain. Assuming well-separated steps, the first two terms are dominating. Therefore, the stability of these surfaces can be evaluated by the sum of the independent free energies of terraces and steps.

While the former contribution can be obtained by calculating a planar Pt(111) surface, the step energies for {111}- and {100}-type step edges were obtained by calculating Pt[5(111) × (111)] [i.e., Pt(355)] and Pt[5(111) × (100)] [i.e., Pt(322)] surfaces from which we subtracted the terrace contributions. In extensive convergence tests these two vicinal Pt surfaces were found to have sufficiently small step-step interactions. Based on this separation in terrace and step contributions the (p,T)-dependent surface free energies were evaluated using the *ab initio* atomistic thermodynamics approach.[26–29]

Since both stepped surfaces, Pt(322) and Pt(355), combine five atom-wide terraces of (111) orientation separated by monoatomic {100} and {111} steps, we used the ratio between step and terrace atoms of 20:80 to define the oxygen coverage at steps Θ_{step}, terraces Θ_{terrace}, and the stepped surface Θ_{tot} by

$$\Theta_{\text{tot}} = \underbrace{0.2\frac{N^{\text{O}}_{\text{step}}}{N^{\text{Pt}}_{\text{step}}}}_{\Theta_{\text{step}}} + \underbrace{0.8\frac{N^{\text{O}}_{\text{terrace}}}{N^{\text{Pt}}_{\text{terrace}}}}_{\Theta_{\text{terrace}}}. \quad (1)$$

III. RESULTS AND DISCUSSION

Figure 1 shows the calculated surface phase diagrams of oxygen-covered Pt(322) and Pt(355) surfaces. The initial stages of adsorption are similar for the two surfaces. In both cases, by increasing $\Delta\mu_{\text{O}}$, the first step sites are occupied (phases b and b′, $\Theta_{\text{step}} = 0.10$ ML). Oxygen adsorption at {100} steps of Pt(322) begins at lower $\Delta\mu_{\text{O}}$ values, which is correlated to the stronger binding energy (BE) of O to {100} rather than {111} steps ($\text{BE}_{\{100\}} = 1.55$ eV vs $\text{BE}_{\{111\}} = 1.45$ eV per O atom). In both cases, oxygen adsorption on the (111) terrace takes place for $\Delta\mu_{\text{O}} \gtrsim -1.20$ eV. The higher onset $\Delta\mu_{\text{O}}$ for terrace adsorption is again related to the weaker BE of O on terraces ($\text{BE}_{(111)} = 1.23$ eV) as compared to steps.

For $\Delta\mu_{\text{O}} \gtrsim -1.0$ eV the order of the adlayer structures becomes considerably different for the two stepped surfaces. On Pt(322), by increasing $\Delta\mu_{\text{O}}$ the step coverage is raised to $\Theta_{\text{step}} = 0.20$ ML (phase d), then subsequently the terrace coverage is increased to $\Theta_{\text{terrace}} = 0.26$ ML ($\Theta_{\text{terrace}} = 0.8\frac{N^{\text{O}}_{\text{terrace}}}{N^{\text{Pt}}_{\text{terrace}}} = 0.8 \times 0.33$ ML $= 0.26$ ML) with a $(\sqrt{3} \times \sqrt{3})R30°$-O adlayer (phase e), and then the maximum step coverage of $\Theta_{\text{step}} = 0.40$ ML (phase f) is reached. This last structure might form as a metastable phase, possibly stabilized due to kinetic limitations in the formation of the PtO_2 bulk oxide. Regarding Pt(355), the saturation step coverage of $\Theta_{\text{step}} = 0.40$ ML is obtained at lower oxygen chemical potentials (phase d′) as compared to Pt(322). It is also noticeable that the structures of the O-covered steps with $\Theta_{\text{step}} = 0.40$ ML differ significantly: At the {111} steps the already mentioned 1D oxide stripes[1] form while the adlayer structure at the {100} steps cannot be assigned to any known Pt-oxide configuration. These results clearly show a preference for oxide formation at {111} steps as compared to {100} ones.

The O 1*s* spectra obtained by XPS experiments on Pt(322) and Pt(355) for oxygen coverages of up to $\Theta_{\text{tot}} \sim 0.88$ ML are shown in Fig. 2. The low coverages were obtained by exposure to oxygen and the higher coverages by exposure to NO_2. We have shown recently[30] that on the clean flat Pt(111) surface an exposure to 20 L oxygen and subsequent annealing to 300 K leads to the formation of a $p(2 \times 2)$ adlayer with a coverage of $\Theta_{\text{tot}} = 0.25$ ML. Interestingly, the same procedure yields an oxygen coverage of approximately $\Theta_{\text{tot}} = 0.33 \pm 0.04$ ML on both stepped surfaces (see Fig. 2). A clear distinction of the respective adsorption sites of oxygen is not possible in the O 1*s* spectra, due to a small chemical shift and a high spectral width.

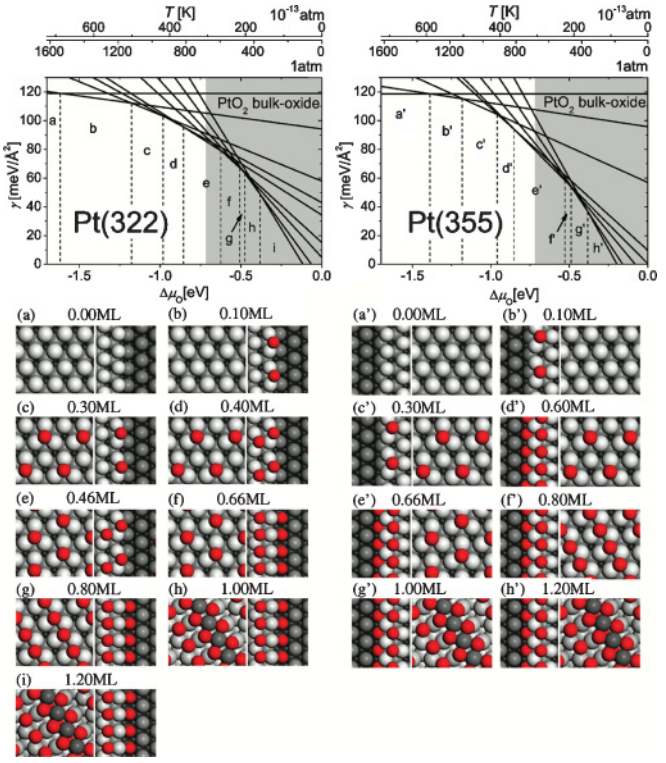

FIG. 1. (Color online) Surface phase diagram for O adsorption on Pt[5(111) × (100)] and Pt[5(111) × (111)], i.e., Pt(322) and Pt(335), showing the total surface free energy as function of the oxygen chemical potential referenced as $\Delta\mu_{\text{O}} = \mu_{\text{O}} - \frac{1}{2}E^{\text{tot}}_{\text{O}_2}$. The dependence on the oxygen chemical potential is converted to temperature scales at 1 atm and typical UHV pressures of 10^{-13} atm. Coverages above each structure model are total coverages Θ_{tot} [see Eq. (1)].

To unequivocally assign the adsorption sites of oxygen to terrace and step sites, we use CO as a probe molecule, which allows to titrate the adsorption sites on the stepped Pt(322) and Pt(355) surfaces. By comparing site-selective measurements of CO adsorption on the O-precovered surfaces with those on the corresponding clean surfaces (see Fig. 3) we analyze the distribution of O on Pt(322) and Pt(355). The temperatures of these coadsorption experiments (140 and 150 K, respectively) were chosen to be sufficiently low to avoid a reaction with the preadsorbed oxygen. All CO coverages are referenced to the $c(4 \times 2)$ CO layer on the planar Pt(111) surface, which has a coverage of 0.50 ML, with 0.25 ML adsorbed at bridge and 0.25 ML at on-top sites.[8]

For the oxygen-free surfaces, the evolution of the total CO coverage presented in Figs. 3(a) and 3(b) indicates that both stepped surfaces have a similar CO saturation coverage:

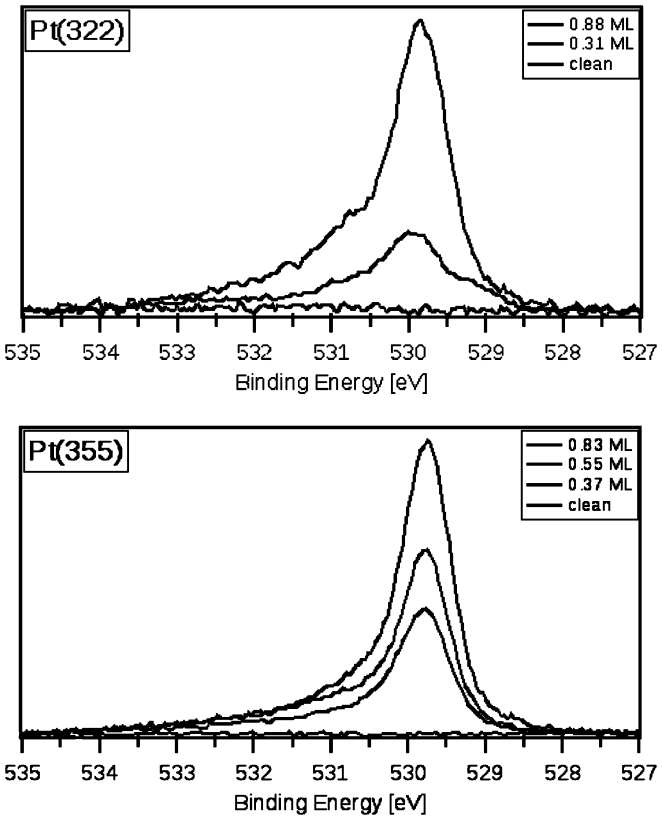

FIG. 2. XPS spectra for the clean and oxygen-covered Pt(322) and Pt(355).

$\Theta_{tot}^{355} \sim 0.5$ ML vs $\Theta_{tot}^{322} \sim 0.52$ ML. The site-resolved analysis in Figs. 3(c) and 3(d) shows that the terrace coverage on Pt(355) ($\Theta_{terrace}^{355} \sim 0.40$ ML) is 0.1 ML smaller than that on Pt(322), while the step coverage on the former ($\Theta_{step}^{355} \sim$ 0.1 ML) is 0.08 ML larger.

For the O-precovered surfaces, the CO saturation coverage is significantly lowered with respect to the clean surfaces [see Figs. 3(a) and 3(b)]. However, the extent of this effect is quite different, indicating a different distribution of the preadsorbed oxygen on the two surfaces. In both cases oxygen preferentially occupies the {100} and {111} step sites on both surfaces [see Figs. 3(c) and 3(d)], which is in accordance with our calculated phase diagram, and thereby blocks completely the adsorption of CO on these sites.

The CO titration on Pt(322) precovered with $\Theta_{tot} =$ 0.31 ML oxygen [Fig. 3(a)] shows the reduction of the CO adsorption ability from ~0.50 to ~0.24 ML on the terrace, indicating that oxygen blocks half of the adsorption sites for CO. Therefore, the oxygen coverage on the terrace is $\Theta_{terrace} = 0.2$ ML. The remaining oxygen, not adsorbed on the terrace, must then be at the step sites: $\Theta_{step} = \Theta_{tot} - \Theta_{terrace} =$ 0.11 ML. The resulting O distribution on the Pt(322) surface is in very good agreement with structure c in Fig. 1.

On Pt(355) with an oxygen coverage of $\Theta_{tot} =$ 0.37 ML, a reduction of the amount of CO from 0.50 to 0.36 ML is observed [see Fig. 3(b)]. Although this reduction is substantially less than in the case of Pt(322), but again an almost complete suppression of the adsorption of CO at the step sites is found [see Fig. 3(d)]. Only small amounts

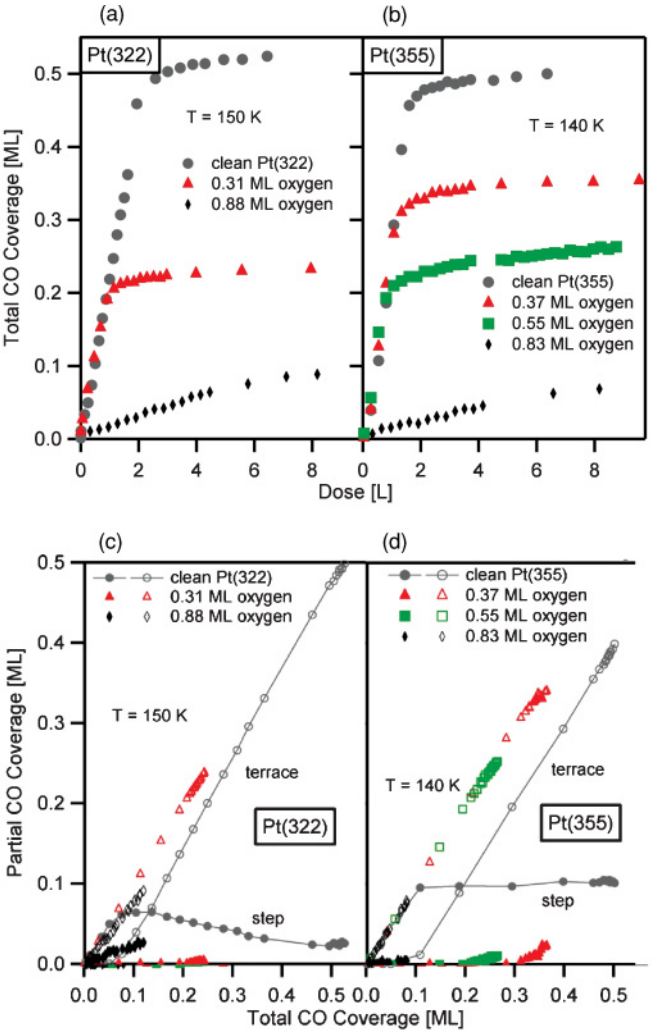

FIG. 3. (Color online) Evolution of the total CO coverage, (a) and (b), and site-resolved analysis, (c) and (d), on stepped Pt(111) for a surface temperature of 150 K.

of CO of up to 0.02 ML are observed at higher exposures, which might be related to either slow CO oxidation or just site exchanges as was observed, e.g., for CO and sulfur.[31] So 0.08–0.1 ML of CO is blocked from the steps and 0.06 ML of CO from terrace sites. Therefore, we conclude that 0.06 ML of O are adsorbed on the terrace, leaving 0.31 ML of oxygen at the steps. For Pt(355) a minor discrepancy between theory and experiment is evident. The former predicts first (with rising chemical potential) an adsorption of $\Theta_{step} = 0.10$ ML of O at the step sites and subsequently an occupation of the terrace sites forming the $p(2 \times 2)$ structure, while in the experiment we do not observe the $p(2 \times 2)$ adlayer but a step coverage that exceeds the $\Theta_{step} = 0.10$ ML. An explanation for this difference could be the fact that the terrace width is still too narrow (10.1 Å) to allow for the establishment of the $p(2 \times 2)$ overlayer structures. On the experimental side the probe molecule used in the experiment could also influence the result, as CO could certainly induce a restructuring of the surface oxygen and the surface itself.

With an oxygen coverage of $\Theta_{tot} = 0.55$ ML on the Pt(355) surface, the CO coverage on the terrace is reduced to 0.25 ML

[(Fig. 3(c), open squares], close to the value expected for the $p(2 \times 2)$-O structure. This reduction from 0.40 to 0.25 ML of CO requires $\Theta_{terrace} = 0.15$ ML oxygen at the terraces. Consequently the remaining oxygen atoms are at the steps ($\Theta_{step} = \Theta_{tot} - \Theta_{terrace} = 0.40$ ML). The proposed experimental structure nicely matches the phase d′ of the phase diagram.

In the calculations an even higher chemical potential of oxygen leads to an increase of O coverage on the terrace of two stepped surfaces with total oxygen coverages of $\Theta_{tot} = 0.80$ ML. Under UHV conditions this coverage can be reached either by using harsh oxidizing conditions or by using a different oxidizing agent, as in our case, NO_2. By exposing the surface to NO_2 at 450 K, a surface oxygen coverage of $\Theta_{tot} \sim 0.8$ ML is achieved. The CO titration experiments show only small amounts of CO on the two surfaces (<0.11 ML), which might be due to defects in the oxygen layer and/or reaction of O with CO, even though the sample is kept at low temperatures. This might be especially true as the highly reactive step sites are populated and the resulting dense, strained oxygen overlayer is less stable. Here DFT is a convenient way to analyze the distribution of oxygen on the surfaces. From a thermodynamic viewpoint, the experimentally observed structures with $\Theta_{tot} \sim 0.8$ ML of oxygen could be phases g and f′ (metastable phases), with the same coverage of 0.4 ML on terrace [$p(2 \times 1)$-O] and at steps.

In the phase diagram we have also considered high-coverage oxygen structures ($\Theta_{tot} = 1.0$ ML and 1.2 ML) forming Pt-oxide chains[32] on flat Pt(111) and $\Theta_{step} = 0.40$ ML of O at steps. In the present experiments, using O_2 and NO_2, dosing of these structures is not reached. Since Devarajan *et al.*[32] have found the Pt-oxide chains on flat Pt(111) by applying oxygen atom beams, we propose that these structures (i.e., h, g′, i, and h′) might be obtained if the formation of the bulk oxide is hindered and/or the surface is exposed to atomic oxygen.

IV. CONCLUSIONS

In conclusion, a combination of DFT calculations and XPS measurements on differently stepped platinum surfaces shows a strong dependence of the adsorption and oxidation behavior on the step orientation. We could show that oxygen adsorption begins at the {100} steps of Pt(322), while the high coverage is reached first at the {111} steps of Pt(355). Although the high-coverage structure at {111} steps is determined to be the experimentally observed 1D oxide stripe, a different oxide structure is found at the {100} steps at high coverages. From our calculations we propose that similar Pt oxide chains could form on the (111) terrace of stepped surfaces at very high coverages, which might indeed be the precursor state for forming surface or bulk oxides. The comparison between experiment and theory showed an encouraging similarity that should allow using DFT calculations for extrapolating surface science results to even higher temperature and pressure regimes, maybe bridging the materials and pressure gap. Also the two methods complemented each other, allowing for more accurate descriptions of the ongoings on the surface.

ACKNOWLEDGMENTS

J.B., P.K., and T.J. gratefully acknowledge support from the "Deutsche Forschungsgemeinschaft" (DFG), the European Union through the Marie-Curie-ITN ELCAT, as well as by the bwGRiD for computing resources. The work performed by the Erlangen authors has been supported by the Cluster of Excellence "Engineering of Advanced Materials," the BMBF through Grant No. 05 ES3XBA/5, and BESSY.

*timo.jacob@uni-ulm.de
†steinrueck@chemie.uni-erlangen.de

[1] J. G. Wang *et al.*, Phys. Rev. Lett. **95**, 256102 (2005).
[2] W. F. Banholzer and R. I. Masel, J. Catal. **85**, 127 (1984).
[3] W. A. Goddard III *et al.*, Mol. Simul. **32**, 251 (2006).
[4] C. Ellinger *et al.*, J. Phys. Condens. Matter **20**, 184013 (2008).
[5] J. M. Hawkins, J. F. Weaver, and A. Asthagiri, Phys. Rev. B **79**, 125434 (2009).
[6] D. H. Parker, M. E. Bartram, and B. E. Koel, Surf. Sci. **217**, 489 (1989).
[7] T. M. Pedersen, W. X. Li, and B. Hammer, Phys. Chem. Chem. Phys. **8**, 1566 (2006).
[8] H. Steininger, S. Lehwald, and H. Ibach, Surf. Sci. **123**, 1 (1982).
[9] J. F. Weaver, J. J. Chen, and A. L. Gerrard, Surf. Sci. **592**, 83 (2005).
[10] P. Legare *et al.*, Surf. Sci. **198**, 69 (1988).
[11] J. Gustafson *et al.*, Phys. Rev. B **74**, 035401 (2006).
[12] B. L. M. Hendriksen *et al.*, Nat. Chem. **2**, 730 (2010).
[13] F. Tao *et al.*, Science **327**, 850 (2010).
[14] R. Westerström *et al.*, Phys. Rev. B **76**, 155410 (2007).
[15] P. R. Norton, J. A. Davies, and T. E. Jackman, Surf. Sci. **122**, L593 (1982).
[16] W. X. Li, J. Phys. Condens. Matter **20**, 184022 (2008).
[17] W. X. Li, L. Osterlund, E. K. Vestergaard, R. T. Vang, J. Matthiesen, T. M. Pedersen, E. Laegsgaard, B. Hammer, and F. Besenbacher, Phys. Rev. Lett. **93**, 146104 (2004).
[18] A. Eichler, F. Mittendorfer, and J. Hafner, Phys. Rev. B **62**, 4744 (2000).
[19] T. Jacob, J. Electroanal. Chem. **607**, 158 (2007).
[20] P. Gambardella, Z. Sljivancanin, B. Hammer, M. Blanc, K. Kuhnke, and K. Kern, Phys. Rev. Lett. **87**, 056103 (2001).
[21] N. Seriani and F. Mittendorfer, J. Phys. Condens. Matter **20**, 184023 (2008).
[22] E. Lundgren *et al.*, J. Phys. Condens. Matter **18**, R481 (2006).
[23] B. Hammer, Top. Catal. **37**, 3 (2006).
[24] The DFT energies for different clean and oxygen-covered Pt surfaces were evaluated using the SEQQUEST code [C. Verdozzi, P. A. Schultz, R. Q. Wu, A. H. Edwards, and N. Kioussis, Phys. Rev. B **66**, 125408 (2002)] with localized basis sets represented by a linear combination of optimized "double-ζ plus polarization" contracted Gaussian functions and norm-conserving pseudopotential, including a nonlinear core correction. The Perdew-Burke-Ernzerhof (PBE)-generalized gradient approximation (GGA) functional was employed to approximate the exchange and correlation energies. The terraces and steps were modeled by unsymmetric seven-layer

slabs. Integrations in reciprocal space were performed on 20×20 (steps) and 5×19 (terraces) Monkhorst-Pack k-point meshes for the 1×1 surface unit cells.

[25]The *in situ* high-resolution XPS measurements were performed at the third-generation synchrotron source BESSY II, Berlin at beamline U49/2 PGM-1 with a transportable setup allowing for fast XPS measurements (below 5 s per spectrum). The overall resolution was set to ∼240 and ∼300 meV, at photon energies of 380 and 650 eV, in the C 1*s* and O 1*s* regions, respectively. This allows to obtain site-resolved information on the adsorbed species [B. Tränkenschuh *et al.*, J. Chem. Phys. **124**, 074712 (2006)].

[26]E. Kaxiras, Y. Bar-Yam, J. D. Joannopoulos, and K. C. Pandey, Phys. Rev. B **35**, 9625 (1987).

[27]M. Scheffler and J. Dabrowski, Philos. Mag. A **58**, 107 (1988).

[28]G.-X. Qian, R. M. Martin, and D. J. Chadi, Phys. Rev. B **38**, 7649 (1988).

[29]K. Reuter and M. Scheffler, Phys. Rev. B **65**, 035406 (2001).

[30]M. Kinne *et al.*, J. Chem. Phys. **120**, 7113 (2004).

[31]R. Streber *et al.*, Chem. Phys. Lett. **452**, 94 (2008).

[32]S. P. Devarajan, J. A. Hinojosa, and J. F. Weaver, Surf. Sci. **602**, 3116 (2008).